

ChemComm

Accepted Manuscript



This is an *Accepted Manuscript*, which has been through the Royal Society of Chemistry peer review process and has been accepted for publication.

Accepted Manuscripts are published online shortly after acceptance, before technical editing, formatting and proof reading. Using this free service, authors can make their results available to the community, in citable form, before we publish the edited article. We will replace this *Accepted Manuscript* with the edited and formatted *Advance Article* as soon as it is available.

You can find more information about *Accepted Manuscripts* in the [Information for Authors](#).

Please note that technical editing may introduce minor changes to the text and/or graphics, which may alter content. The journal's standard [Terms & Conditions](#) and the [Ethical guidelines](#) still apply. In no event shall the Royal Society of Chemistry be held responsible for any errors or omissions in this *Accepted Manuscript* or any consequences arising from the use of any information it contains.

COMMUNICATION

Highly-efficient cocatalyst-free H₂-evolution over silica-supported CdS nanoparticle photocatalysts under visible light

Cite this: DOI: 10.1039/x0xx00000x

Received 00th January 2012,
Accepted 00th January 2012Guiyang Yu,^a Longlong Geng,^a Shujie Wu,^a Wenfu Yan^b and Gang Liu^{*a}

DOI: 10.1039/x0xx00000x

www.rsc.org/

Silica-supported CdS nanoparticle photocatalyst exhibits excellent visible-light driven H₂ evolution activity without the use of a cocatalyst. The apparent quantum yield can reach 42% under 420 nm light illumination.

Semiconductor-based photocatalytic conversion of solar energy to fuels, such as hydrogen, is attracting enormous interest due to its potential contribution to the energy supply and storage.¹⁻⁴ Improving the energy converting efficiency is still a challenging issue for the semiconductor-based photocatalyst, including harvesting longer-wavelength solar light,^{5, 6} improving charge separation and transportation,⁷⁻⁹ and enhancing the reaction efficiency at any given wavelength.¹⁰ Conventionally, cocatalyst is regarded as an important part of the semiconductor-based photocatalyst for H₂ evolution from water splitting.¹¹⁻¹³ Proper loading cocatalyst could enhance the efficiency of photocatalyst via providing trapping sites for the photogenerated charges (promote the charge separation), and serving as redox active sites for hydrogen and oxygen evolution.^{6, 13, 14} However, most of cocatalysts are constructed by noble metal (e.g. Pt, Au, Rh)^{13, 15, 16} or narrow bandgap semiconductor (e.g. RuO₂, IrO₂, MoS₂)^{17, 18} particles. These dark particles inevitably block the light absorption of semiconductors and decrease their capacity to generate electron-hole pairs.^{19, 20} Besides, cocatalyst should be carefully chosen for different semiconductors and the interaction/junction between them needs to be rationally fabricated to facilitate the interfacial charge transportation from semiconductor to cocatalyst.²¹⁻²⁴ Therefore, developing highly efficient cocatalyst-free semiconductor photocatalysts is an ideal and economic subject for their future large-scale application.

Very recently, Schmuki and his co-workers reported a hydrogenation method for preparing cocatalyst-free photocatalysts. They found that anatase TiO₂ hydrogen-treated under 20 bar H₂/Ar stream could be used as a photocatalyst for H₂ evolution without adding any cocatalyst.²⁵ But the high-pressure and strong reduction of hydrogenation process could destroy the structure of some semiconductor, which might limit the applicable scope of this hydrogenation method. Downsize the particles to nanometer could endow semiconductors with many exceptional qualities, including high surface-to-bulk atomic ratio, altered surface energies, quantum confinement effects etc..²⁶⁻²⁸ These features could influence the

charge separation and optical properties of semiconductors. In this work, it was found that CdS nanoparticles dispersed on the surface of mesoporous silica (denoted as CdS@SiO₂) exhibits excellent photocatalytic H₂ evolution activity under visible light irradiation without the use of a cocatalyst. The apparent quantum yield (AQY) can reach 42 % under 420 nm light illumination. To our knowledge, few chalcogenide semiconductor photocatalysts could exhibit such high AQY without cocatalyst. Besides, this strategy and synthesis method is also applicable to prepare other cocatalyst-free metal-sulfide photocatalysts.

A two-step approach was adopted to synthesize CdS@SiO₂ (the experimental details are described in the Supporting Information). First, precursor CdO@SiO₂ was prepared by a sol-gel method in the presence of citric acid. This method has been reported in our previous works to prepare supported nano- TiO₂ and WO₃ materials with high dispersion.²⁹⁻³¹ Citric acid plays an important role in forming mesoporous silica framework and the high dispersion of oxide particles. Second, CdO@SiO₂ was sulfurized in a Na₂S aqueous solution. This synthesis process is based on the principle of solubility product. Anion exchange can easily realize the in-situ conversion of CdO to CdS due to the quite small K_{sp} of CdS (8.0×10⁻²⁷).^{19, 32} The content of CdO in the representative composite is 15 wt%, which was denoted as CdO(15)@SiO₂. The final sulfide material was denoted as CdS(15)@SiO₂.

Fig. 1A shows the X-ray diffraction (XRD) patterns of CdO(15)@SiO₂, CdS(15)@SiO₂, SiO₂ as well as bulk CdO and CdS. Our previous work has shown that SiO₂ prepared with this method possesses amorphous mesoporous structure.³³ Only one broad band from 15° to 30° can be observed. As for CdO(15)@SiO₂, the broad peak at ca. 23° should come from the silica matrix. The shoulder diffraction peak at 32.9° can be ascribed to the (111) plane of monteponite CdO. This peak is relatively broad, indicating that crystallinity of CdO is low and/or the particle size is quite small. CdS(15)@SiO₂ exhibits three diffraction peaks at 2θ = 26.9°, 44.2° and 52.0°, which can be ascribed to (111), (220) and (311) planes of cubic CdS (JCPDS card 80-0019).^{32, 33} The N₂ adsorption-desorption isotherms show that CdS(15)@SiO₂ possess mesoporous characteristics with pore size distributions in a range of 6-14 nm (Fig. 1B). The specific surface area of CdS(15)@SiO₂ is 296 m²g⁻¹ (Table S1).

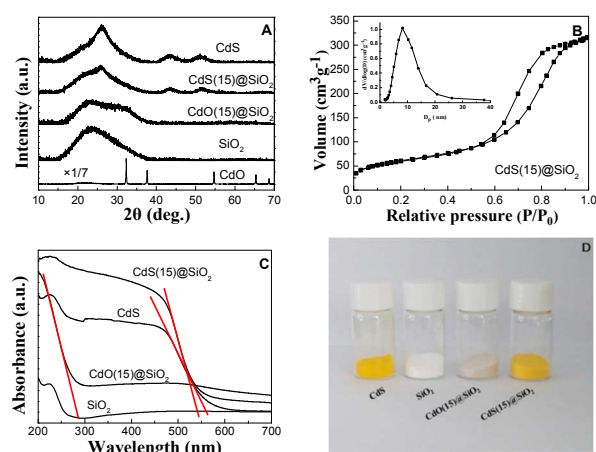


Fig. 1 (A) XRD patterns of CdS(15)@SiO₂, CdO(15)@SiO₂, CdS, CdO, and SiO₂; (B) N₂ adsorption-desorption isotherms and BJH pore size distribution (inset) of CdS(15)@SiO₂; (C) UV-vis diffuse reflection spectra and (D) Photographs of CdS(15)@SiO₂, CdO(15)@SiO₂, SiO₂ and CdS.

UV-vis diffuse reflectance spectra (Fig. 1C) show that CdS(15)@SiO₂ exhibit a strong absorption onset at 550 nm, corresponding to the bandgap (E_g) of about 2.3 eV. In comparison to pure CdS, the absorption edge of CdS(15)@SiO₂ is much sharper. It should be noted that SiO₂ exhibits only weak absorption in deep UV region and no obvious absorption in the range larger than 280 nm. It means that visible light and most of UV light could irradiate guest semiconductors incorporated inside of silica matrix.

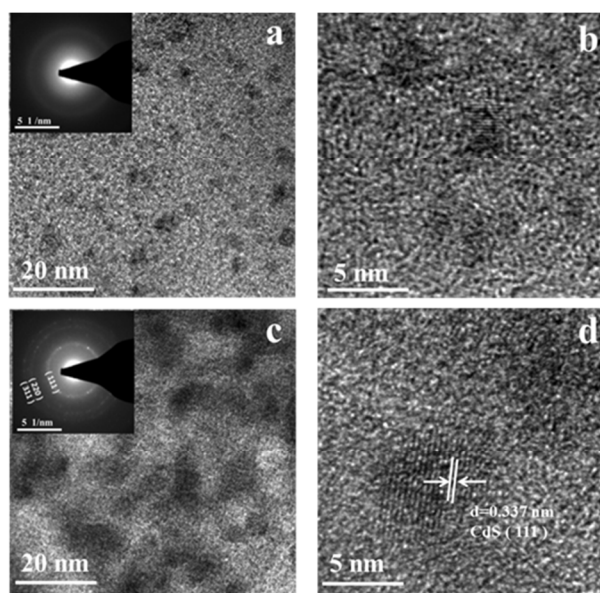


Fig. 2 HRTEM images of CdO(15)@SiO₂ (a and b) and CdS(15)@SiO₂ (c and d).

Fig. 2 shows transmission electron microscopy (TEM) images of CdO(15)@SiO₂ and CdS(15)@SiO₂ at different magnification. The CdO present as *ca.* 4 nm nanoparticle well dispersed on the silica surface (Fig. 2a, S1a and S1b). The high-resolution TEM (HRTEM) image (Fig. 2b) and the selected area electron diffraction (SAED) pattern (inset in Fig. 2a) show that CdO should be amorphous due to no clear lattice fringe and diffraction rings can be seen. As for

CdS(15)@SiO₂, relatively large particles about 8-10 nm can be observed (Fig. 2c, S1c and S1d). The lattice fringe with *d* spacing of 0.337 nm is ascribed to the (111) plane of cubic CdS (Fig. 2d). The SAED pattern indicated that these nanoparticles are polycrystalline. The three inside diffraction rings correspond to the (111), (220), (311) planes of cubic CdS, which is consistent with the XRD results.

The photocatalytic H₂ evolution performance of CdS(15)@SiO₂ was investigated with SO₃²⁻ and S²⁻ as sacrificial reagent under visible light irradiation (the detailed procedures are described in the Supporting Information). Typically, 0.1 g catalyst powder was dispersed in 100 mL aqueous solution containing Na₂S (0.35 M) and Na₂SO₃ (0.25 M). Without adding any cocatalyst, CdS(15)@SiO₂ exhibits a H₂ evolution rate of 831 μmol·h⁻¹, which is much higher than that of bulk CdS (173 μmol·h⁻¹) (Fig. 3A). Long-time test shows that the activity of CdS(15)@SiO₂ has no obviously changed in the continuous 10 h reaction (Fig. S2). XRD and XPS characterizations show that the crystallization and surface chemical state of used sample are similar to the fresh one, suggesting that CdS(15)@SiO₂ is stable in the reaction process (Fig. S3). The quantum yield of CdS(15)@SiO₂ under above reaction condition is 27 % at 420 nm. This value can be further optimized by increasing the amount of CdS(15)@SiO₂ photocatalyst (see in Fig. S4). When the amount of CdS(15)@SiO₂ increases to 0.3 g, The quantum yield at 420 nm can reach to 42 %, which is a very high apparent quantum yield for chalcogenide semiconductor photocatalysts without cocatalyst. The influence of wavelength on the apparent quantum yield for H₂ evolution was also investigated (Fig. 3B). The apparent quantum decreased with increasing the active wavelength and the lowest value of 0.2 % was detected at 600 nm. It shows that only photons of a wavelength shorter than 600 nm can irradiate the CdS(15)@SiO₂ for photocatalytic H₂ evolution.

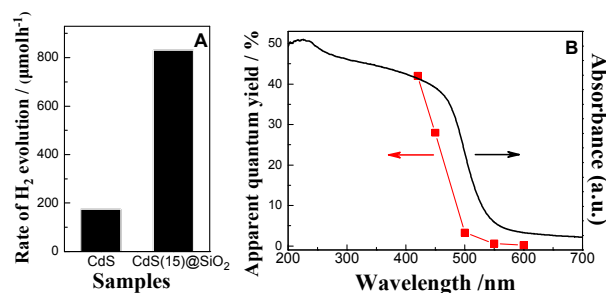


Fig. 3 (A) Photocatalytic H₂ evolution activity of commercial CdS and CdS(15)@SiO₂ under visible light irradiation. Reaction condition: 0.1 g photocatalysts in 100 mL Na₂S (0.35 M)-Na₂SO₃ (0.25 M) solution, 300 W Xe-lamp equipped with cut-off filter ($\lambda \geq 420$ nm); (B) Influence of wavelength on the apparent quantum yield for hydrogen evolution. Reaction condition: 0.3 g CdS(15)@SiO₂ in Na₂S (0.35 M) and Na₂SO₃ (0.25 M) aqueous solution under various wavelengths of 420, 450, 500, 550, and 600 nm.

The influence of CdS contents in CdS@SiO₂ on the photocatalytic activity was investigated in detail (Fig. 4). The CdS contents were tuned by controlling the value of *x* in the CdO(*x*)@SiO₂ precursor (*x* is the weight percentage of CdO), and the resultant photocatalysts were denoted as CdS(*x*)@SiO₂. With increasing *x* from 1 to 50, the H₂ evolution rate of the samples gradually increased, reaching a maximum value of 831 μmol·h⁻¹ at *x* = 15. Further increasing CdS contents, decrease of the catalytic activity can be observed, which should be due to the increase of particle sizes. A relatively well crystallization of cubic CdS can be observed from XRD pattern when *x* value is larger than 20 (Fig. S5).

And their absorption edge shifts to the relatively high wavelength (Fig. S6).

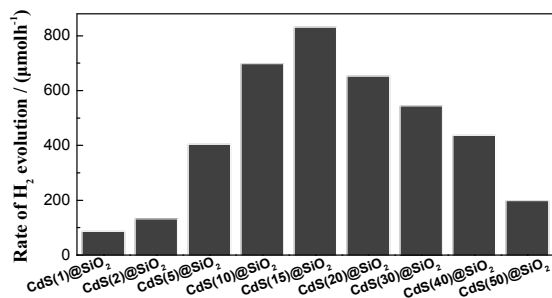


Fig. 4 Photocatalytic H₂ evolution activity of CdS@SiO₂ with different CdS contents under visible light irradiation. Reaction condition: 0.1 g photocatalysts in 100 mL Na₂S (0.35 M)-Na₂SO₃ (0.25 M) solution, 300 W Xe-lamp equipped with cut-off filter ($\lambda \geq 420$ nm).

CdS@SiO₂ could act as highly efficient cocatalyst-free photocatalysts should be attributed to the nanostructure of CdS. It is known that bulk CdS without cocatalyst exhibit relatively low photocatalytic activity for H₂ evolution under the visible light irradiation.^{23, 34} The photoexcited electrons and holes generated within bulk semiconductor have to travel a long distance to the surface to react with water. These electrons and holes may recombine or become trapped at bulk defect sites during this long trip to the surface, which reduce their hydrogen evolution efficiency. As for supported CdS nanoparticles, photoexcited electrons and holes can reach the surface without encountering obstructions due to the ultrafine particle size and high crystallinity.

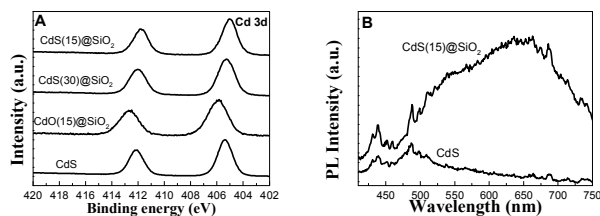


Fig. 5 (A) Cd 3d XPS spectra of the CdS, CdO(15)@SiO₂, CdS(15)@SiO₂ and CdS(30)@SiO₂. (B) PL spectra of CdS and CdS(15)@SiO₂ samples. the excitation wavelength for the emission spectra was 390 nm.

The nanostructure often causes different surface properties from bulk materials. The chemical states of Cd on the surface of CdO(15)@SiO₂, CdS(15)@SiO₂, CdS(30)@SiO₂ and bulk CdS were determined by X-ray photon spectroscopy (XPS, Fig. 5A). Cd (3d) core level is split into Cd 3d_{5/2} and Cd 3d_{3/2} due to spin orbit coupling. The main photoemission lines in the Cd 3d spectrum recorded from CdS(15)@SiO₂ and CdS(30)@SiO₂ appear at lower binding energy than those of the spectrum of bulk CdS, indicating the surface Cd oxidation state of CdS@SiO₂ is lower than that of bulk CdS. This result reflects that a specific defect configuration formed on the surface of CdS nanoparticle. Photoluminescence spectra further confirm the presence of defects on the surface of CdS(15)@SiO₂ (Fig. 5B). The peak centered at 490 nm can be assigned to the band-edge emission of CdS. Comparing with the spectrum of bulk CdS, the largely Stokes-shifted emissions can be observed in the spectrum of CdS(15)@SiO₂. In general, photoexcited electron and hole in semiconductor recombine each

other through several recombination processes such as direct band-to-band coupling and/or shallowly/deeply trapped potential states. Defect sites existing on the surface of semiconductor nanocrystal typically provide deeply trapped potential states which induce largely Stokes-shifted emissions.²⁶

Surface defects usually play positive roles in photocatalytic process.³⁴⁻³⁶ It could serve as an electron collector and transporter to separate the photogenerated electron-hole pairs, effectively lengthening the lifetime of the charge carriers.^{37, 38} With widely studied TiO₂ as example, defects of Ti³⁺ and/or oxygen vacancies could induce a band of electronic states below the conduction band, which facilitates the transport of photocarriers to the surface active sites and responsible for the enhancement of photoactivity.^{39, 40} In our case, the specific surface defect configuration of CdS@SiO₂ should have a direct correlation with the high photocatalytic performance without the use of a cocatalyst. The uniform surface defects on the CdS nanoparticles could form an efficient inner electric field in the particle. According to the theory and practice of TiO₂,^{37-39, 41, 42} the potential of defects should be a little less negative than the conduction band level of CdS. This could lead the photogenerated electrons highly prone to reaching the surface of the photocatalysts and reacting with H⁺ (Fig. 6).

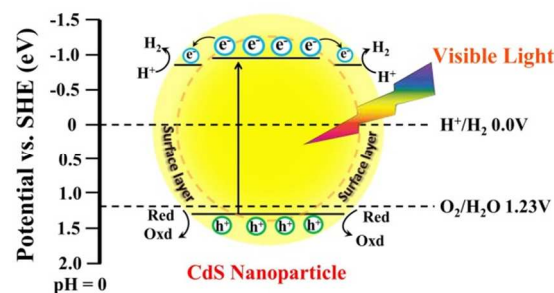


Fig. 6 Schematic illustration of the charge separation and transfer in the CdS nanoparticle of CdS@SiO₂ composite under visible light.

Besides, a large surface area and mesoporous structure are also critical factors for fabricating high-efficiency photocatalysts.^{43, 44} It could enhance the light absorption of CdS and offer more photocatalytic reaction centers. The interconnected uniform-size mesopores could facilitate the diffusion of reagent and H₂ evolution. This strategy and synthesis method is also applicable to prepare other supported metal-sulfide composites, including CdInS₂@SiO₂, ZnInS₂@SiO₂, CuInS₂@SiO₂, In₂S₃@SiO₂, and ZnInCuAgS_x@SiO₂. They also exhibit relatively high photocatalytic H₂ evolution efficiency under visible light irradiation without using additional cocatalysts (see in Fig. S7-S9).

In summary, silica-supported CdS nanoparticle photocatalyst was prepared by a two-step approach, and exhibited excellent photocatalytic H₂ evolution activity under visible light without the use of a cocatalyst. The apparent quantum yield is 42 % under 420 nm light irradiation. The specific surface defect as well as small particle size created an inner driving force, facilitating the photoexcited charges transfer to surface and forming an efficient intrinsic co-catalytic H₂ evolution activity on CdS particle. This work not only provides a general strategy for obtaining cocatalyst-free metal-sulfide photocatalysts but also may open a door for the development of highly efficient water splitting photocatalysts.

The authors acknowledge supports from the National Natural Science Foundation of China (21473073), the Development Project of Science and Technology of Jilin Province

(20130101014JC), the Fundamental Research Funds for the Central Universities and the Open Project of State Key Laboratory of Inorganic Synthesis and Preparative Chemistry.

Notes and references

^a Key Laboratory of Surface and Interface Chemistry of Jilin Province, College of Chemistry, Jilin University, Jiefang Road 2519, Changchun, 130012, China. E-mail: lgang@jlu.edu.cn

^b State Key Laboratory of Inorganic Synthesis and Preparative Chemistry, College of Chemistry, Jilin University, Qianjin Road 2599, Changchun, 130012, China.

† Electronic Supplementary Information (ESI) available: details of the synthesis, characterization, photocatalytic activity measurement, and additional figures. See DOI: 10.1039/c000000x

- A. Kudo and Y. Miseki, *Chem. Soc. Rev.*, 2009, **38**, 253-278.
- K. Maeda, K. Teramura, D. Lu, T. Takata, N. Saito, Y. Inoue and K. Domen, *Nature*, 2006, **440**, 295.
- X. B. Chen, S. H. Shen, L. J. Guo and S. S. Mao., *Chem. Rev.*, 2010, **110**, 6503-6570.
- J. Zhao, T. Minegishi, L. Zhang, M. Zhong, Gunawan, M. Nakabayashi, G. Ma, T. Hisatomi, M. Katayama, S. Ikeda, N. Shibata, T. Yamada and K. Domen, *Angew. Chem. Int. Ed.*, 2014, **53**, 11808-11812.
- A. Tanaka, K. Fuku, T. Nishi, K. Hashimoto and H. Kominami, *J. Phys. Chem. C*, 2013, **117**, 16983-16989.
- A. Tanaka, K. Hashimoto and H. Kominami, *J. Am. Chem. Soc.*, 2014, **136**, 586-589.
- X. Wang, Q. Xu, M. R. Li, S. Shen, X. L. Wang, Y. C. Wang, Z. C. Feng, J. Y. Shi, H. X. Han and C. Li, *Angew. Chem. Int. Ed.*, 2012, **51**, 13089-13092.
- A. M. Smith and S. Nie, *Acc. Chem. Res.*, 2010, **43**, 190-200.
- X. Wang, G. Liu, Z. G. Chen, F. Li, L. Wang, G. Q. Lu and H. M. Cheng, *Chem. Comm.*, 2009, 3452-3454.
- C.-T. Dinh, H. Yen, F. Kleitz and T.-O. Do, *Angew. Chem. Int. Ed.*, 2014, **126**, 6736-6741.
- J. Fang, L. Xu, Z. Zhang, Y. Yuan, S. Cao, Z. Wang, L. Yin, Y. Liao and C. Xue, *ACS Appl. Mater. Interfaces*, 2013, **5**, 8088-8092.
- M. Murdoch, G. I. Waterhouse, M. A. Nadeem, J. B. Metson, M. A. Keane, R. F. Howe, J. Llorca and H. Idriss, *Nat. Chem.*, 2011, **3**, 489-492.
- K. Wu, Z. Chen, H. Lv, H. Zhu, C. L. Hill and T. Lian, *J. Am. Chem. Soc.*, 2014, **136**, 7708-7716.
- D. W. Jinhui Yang, Hongxian Han, Can Li, *Acc. Chem. Res.*, 2013, **46**, 1900-1909.
- M. Yoshida, K. Maeda, D. Lu, J. Kubota and K. Domen, *J. Phys. Chem. C*, 2013, **117**, 14000-14006.
- X. Yu, A. Shavel, X. An, Z. Luo, M. Ibanez and A. Cabot, *J. Am. Chem. Soc.*, 2014, **136**, 9236-9239.
- F. Lin, D. Wang, Z. Jiang, Y. Ma, J. Li, R. Li and C. Li, *Energy & Environ. Sci.*, 2012, **5**, 6400-6406.
- X. Zong, H. Yan, G. Wu, G. Ma, F. Wen, L. Wang and C. Li, *J. Am. Chem. Soc.*, 2008, **130**, 7176-7177.
- N. Bao, L. Shen, T. Takata and K. Domen, *Chem. Mater.*, 2008, **20**, 110-117.
- D. Wang, T. Hisatomi, T. Takata, C. Pan, M. Katayama, J. Kubota and K. Domen, *Angew. Chem. Int. Ed.*, 2013, **52**, 11252-11256.
- K. Iwashina, A. Iwase, Y. H. Ng, R. Amal and A. Kudo, *J. Am. Chem. Soc.*, 2015, **137**, 604-607.
- M. Liu, F. Li, Z. Sun, L. Ma, L. Xu and Y. Wang, *Chem. Comm.*, 2014, **50**, 11004-11007.
- T. Peng, X. Zhang, P. Zeng, K. Li, X. Zhang and X. Li, *J. Catal.*, 2013, **303**, 156-163.
- T. Simon, N. Bouchonville, M. J. Berr, A. Vaneski, A. Adrović, D. Volbers, R. Wyrwich, M. Döblinger, A. S. Susha, A. L. Rogach, F. Jäckel, J. K. Stolarczyk, and J. Feldmann, *Nat. Mater.*, 2014, **13**, 1013-1018.
- N. Liu, C. Schneider, D. Freitag, U. Venkatesan, V. R. Marthala, M. Hartmann, B. Winter, E. Spiecker, A. Osvet, E. M. Zolnhofer, K. Meyer, T. Nakajima, X. Zhou and P. Schmuki, *Angew. Chem. Int. Ed.*, 2014, **53**, 14201-14205.
- W.-S. Chae, S.-W. Lee, M.-J. An, K.-H. Choi, S.-W. Moon, W.-C. Zin, J.-S. Jung and Y.-R. Kim, *Chem. Mater.*, 2005, **17**, 5651-5657.
- L. Liao, Q. Zhang, Z. Su, Z. Zhao, Y. Wang, Y. Li, X. Lu, D. Wei, G. Feng, Q. Yu, X. Cai, J. Zhao, Z. Ren, H. Fang, F. Robles-Hernandez, S. Baldelli and J. Bao, *Nat. Nanotech.*, 2014, **9**, 69-73.
- M. D. Peterson, S. C. Jensen, D. J. Weinberg, and E. A. Weis, *ACS Nano*, 2014, **8**, 2826-2837.
- G. Liu, Y. Liu, G. Yang, S. Li, Y. Zu, W. Zhang and M. Jia, *J. Phys. Chem. C*, 2009, **113**, 9345-9351.
- G. Liu, X. Wang, X. Wang, H. Han and C. Li, *J. Catal.*, 2012, **293**, 61-66.
- G. Liu, J. F. Han, X. Zhou, L. Huang, F. X. Zhang, X. L. Wang, C. M. Ding, X. J. Zheng, H. X. Han and C. Li, *J. Catal.*, 2013, **307**, 148-152.
- Q. Li, B. Guo, J. Yu, J. Ran, B. Zhang, H. Yan and J. R. Gong, *J. Am. Chem. Soc.*, 2011, **133**, 10878-10884.
- Y. Li, H. Wang and S. Peng, *J. Phys. Chem. C*, 2014, **118**, 19842-19848.
- J. Zhang, Q. Xu, Z. Feng, M. Li and C. Li, *Angew. Chem. Int. Ed.*, 2008, **120**, 1790-1793.
- X. Wang, Q. Xu, F. T. Fan, X. L. Wang, M. R. Li, Z. C. Feng and C. Li, *Chem. Asian J.*, 2013, **8**, 2189-2195.
- X. Wang, S. Shen, J. S. Jin, J. X. Yang, M. R. Li, X. L. Wang, H. X. Han and C. Li, *Phys. Chem. Chem. Phys.*, 2013, **15**, 19380-19386.
- X. Pan, M. Q. Yang, X. Fu, N. Zhang and Y. J. Xu, *Nanoscale*, 2013, **5**, 3601-3614.
- X. Yu, B. Kim and Y. K. Kim, *ACS Catal.*, 2013, **3**, 2479-2486.
- X. Chen, L. Liu, P. Y. Yu and S. S. Mao, *Science*, 2011, **331**, 746-750.
- Y. H. Hu, *Angew. Chem. Int. Ed.*, 2012, **51**, 12410-12412.
- M. Liu, L. Wang, G. Lu, X. Yao and L. Guo, *Energy & Environ. Sci.*, 2011, **4**, 1372.
- H. Yaghoubi, Z. Li, Y. Chen, H. T. Ngo, V. R. Bhethanabotla, B. Joseph, S. Ma, R. Schlaf and A. Takshi, *ACS Catal.*, 2015, **5**, 327-335.
- W. Li, Z. Wu, J. Wang, A. A. Elzatahry and D. Zhao, *Chem. Mater.*, 2014, **26**, 287-298.
- Y. P. Xie, Z. B. Yu, G. Liu, X. L. Ma and H.-M. Cheng, *Energy & Environ. Sci.*, 2014, **7**, 1895-1901.